Proceedings of the 17th World Congress
The International Federation of Automatic Control
Seoul, Korea, July 6-11, 2008

Robust torque tracking control for E-IVT hybrid powertrain

O. REYSS [*, **] **G. DUC** [*] **P. POGNANT-GROS** [**]
G. SANDOU [*]

[*] *Automatic Control Department, SUPELEC, 3 rue Joliot Curie, 91192 Gif-sur-Yvette, France (e-mail: olivier.reyss@supelec.fr, gilles.duc@supelec.fr, guillaume.sandou@supelec.fr)*
[**] *Renault Advanced Engineering Department, avenue du golf, 78288 Guyancourt, France (e-mail: philippe.pognant-gros@renault.com)*

Abstract: This study deals with the control of a hybrid vehicle powertrain, composed of three actuators (one engine, two electric machines). This powertrain belongs to the Electric-Infinitely Variable Transmission (E-IVT) class. In order to achieve low fuel consumption, drivability and electric power management, controllers have to achieve simultaneously three specifications, namely engine speed, wheel-torque and battery power references. Decoupled controlled-output behaviors and optimal performances are also required.
In order to imitate a classical powertrain, the control structure is split in two parts. The interest is to decouple transmission speed ratio control and wheel torque control. A model-based design approach is proposed, that directly deals with robustness and decoupling, in a full multivariable and frequency-dependent framework (H_∞ synthesis).
Closed-loop simulations are presented. Stability and performances subject to disturbances and non-linearities are also evaluated, using the theory of linear parameter varying (LPV) systems.

Keywords: H_∞-synthesis; Linear Parameter Varying Systems; Hybrid electric powertrain

1. *INTRODUCTION*

The development of new automotive engine and powertrain concepts is driven by the aim to reduce the average fleet CO_2 emissions and fuel consumption. Hybrid powertrain concepts, in addition to the conventional internal combustion engine (ICE), are equipped with one or more electrical machines and a battery as an energy storage unit. By using the specific advantages of both power sources, hybrid vehicles are considered as a short term possibility to achieve the mentioned goals (see Chan et al. (2001) and Larminie et al. (2003)). The study deals with the control of a dual-mode power-split hybrid powertrain. It is composed of three actuators (one ICE, two electric machines) which allow managing the power from the engine and the battery to the wheels. Opening or closing breaks change speed ratios between actuators and wheels, resulting in two different mechanical modes. This structure has been presented by Villeneuve (2004). Many algorithms have been developed to determinate efficient references, in order to achieve low fuel consumption, drivability and electric power management (see Chau et al. (2002) and Hofman et al. (2005)). Then, specifications are: engine speed, wheel torque and battery power references, decoupling the controlled-output behaviors and achieving optimal closed-loop performances subject to uncertainties or non-linearities. This powertrain is described in section 2.

To enable the design of the control law, a complete model of the system has been defined. Its study showed that it is possible to perform reduction without losing accuracy on its behavior. It also showed non-linearities due to battery charge process. Indeed, our system can be written as a quasi-LPV (linear parameter varying) model, which means that matrices of its state-space description are time-varying. Although stability and performances of our system could seriously be degraded by this non-linearity, a linear time invariant controller has been designed. Thus, it would be easier to embed the controller into a prototype and to tune it. As a result, the stability and performance robustness subject to such variations has to be guaranteed.

To imitate a classical powertrain control, the control structure has been split in two parts, decoupling transmission speed ratio and wheel torque controls. As shown in section 3, this new control law is composed of two controllers : a 2×2-multivariable part, controlling ICE speed and battery power, and an open-loop part, controlling wheel torque. To design the closed-loop part of the control structure, a model-based design approach is proposed, that directly deals with robustness and decoupling, in a full multivariable and frequency-dependent framework. It is based on H_∞ synthesis. All the design specifications can be expressed by frequency-dependent weights on different closed-loop transfers. This approach allows fixing compromises between each closed-loop objectives and is presented in section 4. Robust stability and performances subject to disturbances and non-linearities have been analysed in section 5. Stability and performances of the non-linear system are then analysed by applying the LPV systems theory. It gave good results. Closed-loop simulations on a model of the vehicle are then performed. Since the results detailed in section 6 are very convincing, this control law will be implemented into a prototype.

2. SYSTEM DESCRIPTION

2.1 Structure

The main advantage of this structure (figure 1) is the possibility to operate in two mechanical modes. The first one stands for low speeds, the second for high speeds. This dual-mode structure allows reducing the electric machine's maximal power. Furthermore, different driving conditions imply different control strategies. For example, it may be interesting to track the wheel torque (as a classic car does), whereas it may be better to keep the engine speed at zero in particular situations. This structure is presented in Villeneuve (2004). In this study, the first mechanical mode and the torque tracking strategy will only be considered.

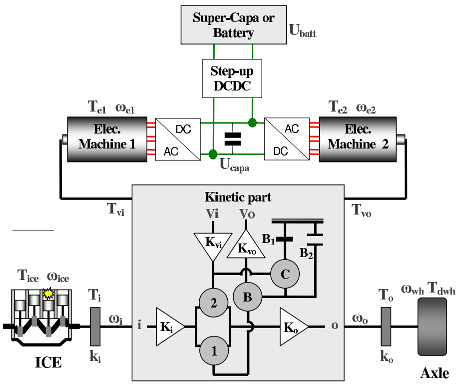

Fig. 1. Mechanical structure of the system in the first mode

On this scheme (torques being in $N.m$, speeds in $rad.s^{-1}$ and voltage in V):

- T_{e1} and ω_{e1} (respectively T_{e2} and ω_{e2}) are machine 1 (resp. 2) torque and speed,
- T_{ice} and ω_{ice} are the torque and speed of the Internal Combustion Engine (ICE),
- T_{dice} is the friction torque of the ICE (as well as disturbances on the ICE shaft)
- T_{dwh} and ω_{wh} are the wheel torque and speed,
- k_i (respectively k_o) is the stiffness of the axle that links the ICE to the powertrain (resp. the axle that links the wheels to the powertrain),
- T_i and ω_i is the torque and speed of the axle that links the ICE to the powertrain,
- T_o and ω_o is the torque and speed of the axle that links the wheels to the powertrain,
- T_{vi} and ω_{vi} is the torque and speed of the axle that links the electric machine 1 to the powertrain,
- T_{vo} and ω_{vo} is the torque and speed of the axle that links the electric machine 2 to the powertrain,
- U_{capa} is the electric machines input voltage (and E_{capa} for the battery charge level),
- U_{batt} is the battery voltage,
- $\mathcal{P}_{dcdc}$ (in W) is the power (either positive or negative) transmitted from the super-capacitor to the buffer-capacitor (by the DC/DC converter) added to the electric losses (electric machines and converter),
- M is a matrix that links ω_i, ω_o, ω_{vi} and ω_{vo}

According to figure 1, the kinetic part is composed of four planetary trains (1, 2, B and C), two breaks B1 and B2, and four speed ratios K_i, K_o, K_{vi} and K_{vo}. It is connected to the ICE, to the wheels and to the electric machines 1 and 2. The electrotechnical part operates as follows: both machines are connected to a buffer-capacitor via two converters. The aim of this capacitor is not power storage but ensuring a convenient voltage at the machines input. A super-capacitor stands for power storage. Both capacitors are connected by a step-up DC/DC converter. The high bandwidth of the electric machines allows controlling the buffer-capacitor voltage. Studying the transmission, the buffer-capacitor is only considered. Then, the super-capacitor and the DC/DC converter can be seen as positive or negative power stream.

The aim of this study is to design an appropriate controller for this system whose aim is to track references for the wheel torque $T_o^\sharp$, the ICE speed $\omega_{ice}^\sharp$ and the electric machines power $E_{capa}^\sharp$ by generating control inputs (T_{e1}, T_{e2} and T_{ice}) for both electric machines and for the ICE. In order to design a controller for the system, the set of specifications for the first mechanical mode and the torque tracking strategy is as follows:

(1) time response ($\tau_{\omega ice}$) smaller than a predetermined value for ω_{ice};
(2) time response (τ_{T_o}) smaller than a predetermined value for T_o;
(3) U_{capa} in a range centered on its nominal value U_{capa}^{ref};
(4) good stability margins;
(5) reduced actuators activity;
(6) controlled-output behaviors decoupling;
(7) rejection of main disturbances (T_{dice}, T_{dwh} and $\mathcal{P}_{dcdc}$).

Studying each component behavior, a full-order model is obtained. Neglecting high frequency dynamics, the model has been reduced to a 3 states model. Its state space description is as follows:

$$\begin{bmatrix} \dot{\omega_{e1}} \\ \dot{\omega_{e2}} \\ \dot{E}_{capa} \end{bmatrix} = A \begin{bmatrix} \omega_{e1} \\ \omega_{e2} \\ E_{capa} \end{bmatrix} + \begin{bmatrix} B_{11} & B_{12} & B_{13} \\ B_{21} & B_{22} & B_{23} \\ -\omega_{e1} & -\omega_{e2} & 0 \end{bmatrix} \begin{bmatrix} T_{e1} \\ T_{e2} \\ T_{ice} \end{bmatrix} + \qquad (1)$$

$$+ \begin{bmatrix} B_{d11} & B_{d12} & 0 \\ B_{d21} & B_{d22} & 0 \\ 0 & 0 & 1 \end{bmatrix} \begin{bmatrix} T_{dice} \\ T_{dwh} \\ \mathcal{P}_{dcdc} \end{bmatrix}$$

$$\begin{bmatrix} \omega_{ice} \\ E_{capa} \\ T_o \end{bmatrix} = \begin{bmatrix} C \\ C_{T_o} \end{bmatrix} \begin{bmatrix} \omega_{e1} \\ \omega_{e2} \\ E_{capa} \end{bmatrix} + \begin{bmatrix} D & & 0 \\ D_{T_o1} & D_{T_o2} & D_{T_o3} \end{bmatrix} \begin{bmatrix} T_{e1} \\ T_{e2} \\ T_{ice} \end{bmatrix} +$$

$$+ \begin{bmatrix} 0 & 0 & 0 \\ 0 & 0 & 0 \\ D_{d31} & D_{d32} & 0 \end{bmatrix} \begin{bmatrix} T_{dice} \\ T_{dwh} \\ \mathcal{P}_{dcdc} \end{bmatrix}$$

Where A, each B_{ij}, C_{ij} and D_{ij} are constant matrices that depends on the mechanical structure of the transmission. Three disturbances in the reduced model have to be considered: T_{dice}, T_{dwh} and $\mathcal{P}_{dcdc}$ for the energetic part.

2.2 System properties

The equation describing the energetic part of the system contains torque/speed products. A LPV (linear parameter varying) system is a system whose state space description matrices depend on varying parameters. The system (1) is not exactly a LPV system: one matrix is linearly dependent on ω_{e1} and ω_{e2}, but these parameters are also states of the system. Such systems are called quasi-LPV systems. An equivalent LPV system can be obtained by considering ω_{e1} and ω_{e2} both as state variables and varying parameters having the same variation range and dynamics. Helmersson (1995) and Leith et al. (2000) show that properties satisfied by the equivalent LPV system are satisfied by the quasi-LPV system (but the converse is not true). As soon as arbitrary variations are considered for the equivalent LPV, variations of the states ω_{e1} and ω_{e2} are a subset of variations of the equivalent LPV parameters. It means that tools developed for LPV systems can be applied to the system, although it is somewhat conservative.

3. *CONTROL STRUCTURE*

3.1 Global control structure

The controller is a MIMO controller, whose inputs are references $T_o^\sharp$, $\omega_{ice}^\sharp$ and $E_{capa}^\sharp$, and each measure delivered by the system, that is to say E_{capa}, ω_{e1} and ω_{e2} (see figure 2). Note that it is possible to compute ω_{ice} as $\omega_{ice} = [\,1\ \ 0\,]\, M \begin{bmatrix} \omega_{e1} \\ \omega_{e2} \end{bmatrix}$.

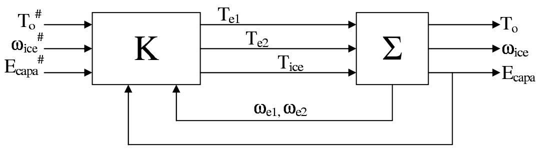

Fig. 2. Classic control structure

3.2 Structure proposal for the controller

The strategy of figure 2 is fully multivariable. As a result, this control law may be totally different from the one used in a classic vehicle, that is split in two independent but communicating parts: one that tracks the speed ratio between the ICE and the wheels (gear box control) and another that tracks the wheel torque (ICE control). Usually, a mechanic gear box operates in a discrete mode, but when the car is taking off, its behavior is close to an IVT's one (so does a robotized gear box changing its speed ratio). Indeed, the gear box controller or the driver continuously operates on the speed ratio with the clutch. It would be interesting to get profit of such a knowledge by designing a two levels control structure: a first level tracking the wheel torque by calculating the ICE torque, and a second one tracking the speed ratio between the ICE and the wheels, with the two electric machines torques.

The study of the system model (1) shows an interesting property. Since C_{T_o} is zero, a simple algebraic equation links six torques: T_o, T_{e1}, T_{e2}, T_{ice}, T_{dice} and T_{dwh}:

$$T_o = D_{T_o1}T_{e1} + D_{T_o2}T_{e2} + D_{T_o3}T_{ice} + D_{d31}T_{dice} + D_{d32}T_{dwh} \qquad (2)$$

It has important consequences on the control law. It shows that it is possible to have a first controller K_1 for ω_{ice} and E_{capa} whose outputs are T_{e1} and T_{e2}, and a second one K_2 tracking T_o using T_{ice}. For the control law to be accurate, $T_o^\sharp$ is considered as a disturbance in the design of the first controller (see figure 3). Considering a classic powertrain,

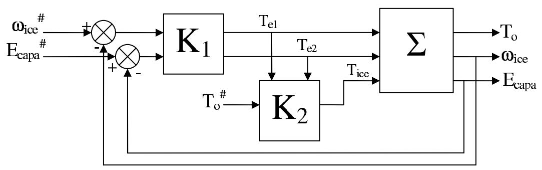

Fig. 3. Control structure proposal

T_{ice} is obtained from $T_o^\sharp$ and estimations of T_{dwh} and T_{dice}. In this paper, we consider $T_o^\sharp = T_o$, and T_{dwh} and T_{dice} as negligible to design K_2, which is described by:

$$T_{ice} = \frac{1}{D_{T_o3}}(T_o^\sharp - D_{T_o1}T_{e1} - D_{T_o2}T_{e2}) \qquad (3)$$

Consider now the design of controller K_1. Substituting equation (3) in model (1), one obtains the following synthesis model:

$$\begin{bmatrix} \dot{\omega}_{e1} \\ \dot{\omega}_{e2} \\ \dot{E}_{capa} \end{bmatrix} = A \begin{bmatrix} \omega_{e1} \\ \omega_{e2} \\ E_{capa} \end{bmatrix} + B' \begin{bmatrix} T_{e1} \\ T_{e2} \end{bmatrix} + B'_d \begin{bmatrix} T_{dice} \\ T_{dwh} \\ \mathcal{P}_{dcdc} \\ T_o^\sharp \end{bmatrix}$$
$$\begin{bmatrix} \omega_{ice} \\ E_{capa} \end{bmatrix} = C \begin{bmatrix} \omega_{e1} \\ \omega_{e2} \\ E_{capa} \end{bmatrix} + D \begin{bmatrix} T_{e1} \\ T_{e2} \end{bmatrix} \qquad (4)$$

with: $B' = \begin{bmatrix} B_{11} - B_{13}\dfrac{D_{T_o1}}{D_{T_o3}} & B_{12} - B_{13}\dfrac{D_{T_o2}}{D_{T_o3}} \\ B_{21} - B_{23}\dfrac{D_{T_o1}}{D_{T_o3}} & B_{22} - B_{23}\dfrac{D_{T_o2}}{D_{T_o3}} \\ -\omega_{e1} & -\omega_{e2} \end{bmatrix}$

and: $B'_d = \begin{bmatrix} B_{d11} & B_{d12} & 0 & \dfrac{B_{13}}{D_{T_o3}} \\ B_{d21} & B_{d22} & 0 & \dfrac{B_{23}}{D_{T_o3}} \\ 0 & 0 & 1 & 0 \end{bmatrix}$

Controller K_1 can be designed by any automatic control method. The main advantage of this structure is the decoupling of two different behaviors: one part of the control law acts as a gear box controller and controls the battery charge, the other part acts as an ICE controller. As explained before, such a control law allows using the knowledge of classic powertrains. Furthermore, it may be very efficient because fast actuators (electric machines) are split from the slow one (ICE).

4. *K1 CONTROLLER SYNTHESIS*

The principle of H_∞ synthesis (see Doyle et al. (1989) and Zhou et al. (1996)) is the minimization of the H_∞ norm of one or several transfers of the system. Such a method allows satisfying sharp specifications as: performances (time response, overshoot), stability margins or actuator limitations, by introducing frequency dependent weights (see figure 4).

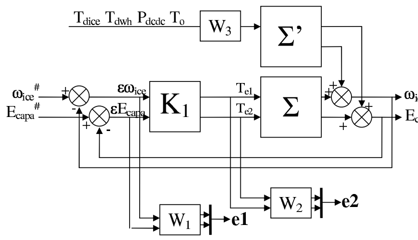

Fig. 4. Closed-loop system with frequency dependent weights

In this study, the aim of H_∞ synthesis tools that have been used is to reduce the H_∞-norm of transfers between references and disturbances, and tracking errors and control inputs, that is to say:

$$\begin{bmatrix} e_1 \\ e_2 \end{bmatrix} := \begin{bmatrix} W_1 S & -W_1 S \Sigma' W_3 \\ W_2 K_1 S & -W_1 K_1 S \Sigma' W_3 \end{bmatrix} \begin{bmatrix} r \\ d \end{bmatrix}$$

Since the matrices of the quasi-LPV model linearly depend on ω_{e1} and ω_{e2}, a polytopic LPV representation can be used: such an approach requires considering that ω_{e1} and ω_{e2} evolve in a convex polygone of $\Re^2$. It will be defined by considering different physical limitations, the first one being the variation ranges $[\omega_{e1min}; \omega_{e1max}]$ and $[\omega_{e2min}; \omega_{e2max}]$. In a simple model of the system (neglecting stiffness of the flywheel and the axles), there is an algebraic relation linking ω_{e1}, ω_{e2}, ω_{ice} and ω_{wh} (so does the vehicle speed V_{vh}). The matrix that links these variables is M. There are limitations on ω_{ice} and V_{vh} too. The main difference between both mechanical modes is the value of M. On the other hand, the first mechanical mode stands for $\omega_{e1} > 0$, and the second mode stands for $\omega_{e1} < 0$. It is possible to draw the two polytopes (for each mode) on the same figure.

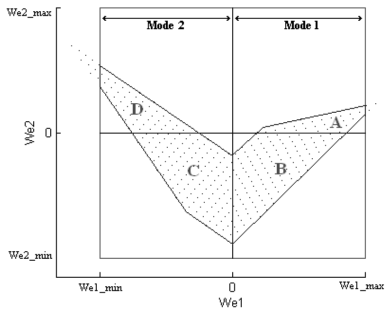

Fig. 5. ω_{e1} and ω_{e2} polytope, considering all limitations

On figure 5, the biggest square stands for the electric machines limitations, dotted areas represent ω_{ice} and V_{vh} limitations and A, B, C and D areas are the intersections of both. As we are studying the first mechanical mode, we only consider the polytope obtained by the union of zones A and B, that is convex.

5. *LTI CONTROLLER - H_∞ SYNTHESIS*

5.1 Synthesis framework

The system being LPV, it is possible to design either a non-linear controller (for example a polytopic LPV controller) or a LTI controller. The choice made in this paper is to design a LTI controller based on the model linearised on a significant operating point of the polytope. Such a controller is easier to tune and more compact. This makes it being easily implementable into a vehicle. The operating point has been iteratively chosen in order to increase performances of the controller subject to variation in the polytope. To validate this choice, stability and performances of such a controller have to be analysed with LPV analysis tools. According to this, conditions to perform the synthesis of a robust controller are:

(1) consider a two levels control structure,

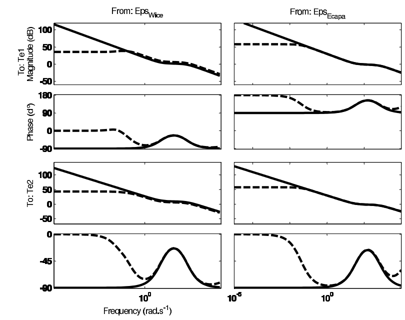

Fig. 6. full-order (dashed line) and simplified (solid line) controllers Bode diagrams

(2) focus on the first mechanical mode, and a torque tracking strategy,
(3) use a linearised model of the system for some operating point,
(4) perform H_∞ synthesis (LMI solver),
(5) design frequency dependent weights induced by specifications: two first order weights W_1 and W_2 are introduced for tracking errors and control inputs, whereas W_3 is chosen as a constant diagonal matrix.

5.2 Reduction and analysis of the controller

According to figure 4 where suitable filters W_i are used for the synthesis procedure, the controller stabilises the system at the corresponding operating point, and ensures that each transfer (between inputs $\omega_{ice}^\sharp$, $E_{capa}^\sharp$, T_{dice}, T_{dwh}, $\mathcal{P}_{dcdc}$, T_o and outputs e_1 and e_2) has an H_∞ norm γ smaller than 1. The controller order is six, this order being imposed by the synthesis algorithm. Often, such a controller contains useless states so that the specifications can be satisfied with a reduced number of states. Furthermore, the final controller must also have an integral behavior at low frequency. In order to simplify the controller, a Hankel singular value (HSV) analysis has been performed. HSV decomposition leads to $\frac{\sigma_3}{\sigma_2} = 213$. It means that we can eliminate four low-controllability / observability states.

Keeping in mind that a reduced-order controller also has to satisfy $\gamma \leq 1$, the controller has been simplified. Each element of the transfer matrix has been simplified to order two, without changing significantly their frequency dependent shape. On the other hand, the synthesis algorithm imposes frequency dependent weights to be proper. Furthermore, stability constraints imposes weights on tracking errors W_1 to have a low frequency pole. This pole stands in the obtained controller, and the lowest the frequency of this pole is, the better the performances are. As a result, it is gainful to substitute such poles by zero poles. Finally, simplified controller K_1 is composed of 4 PI controllers, with high frequency filtering. The order of the simplified controller is four. Figure 6 presents full-order and simplified controllers Bode diagrams. As a result, we will now call $K1$ the simplified controller (tracking ω_{ice} and E_{capa})).

5.3 Controller analysis

The model required to design the controller is different from the real system (that is non-linear). Considering the real system, ω_{e1} and ω_{e2} vary inside the polytope AB of figure 5. Moreover, the whole system is now considered, that's to say the closed-loop part ($K1$, tracking ω_{ice} and E_{capa}, see figure 3) and the open loop part ($K2$, tracking T_o). Every guarantees on stability and performances given by H_∞ synthesis are lost. As a result, the use of stability and performance analysis tools is necessary.

The state space description of the system can be written:

$$\dot{x}_S = A_S x_S + B_S(\theta) u_S$$
$$y = C_S x_S + D_S u_S$$

where A_S, C_S and D_S are constant matrices and B_S is a matrix that linearly depends on $\theta = [\omega_{e1}, \omega_{e2}]$ that is time varying in the polytope $\Theta = AB$. A controller being designed, it is possible to write the state space description of the closed-loop system, named S_{BF}, as:

$$\dot{x} = A(\theta)x + B(\theta)u$$
$$y = C(\theta)x + D(\theta)u$$

where $A(\theta)$, $B(\theta)$, $C(\theta)$ and $D(\theta)$ are varying matrices since they are dependent on B_S.

It is possible to study quadratic stability of the closed-loop system. This study leads to solving LMIs. Becker et al. (2005) and Gahinet et al. (1996) showed that quadratic stability is satisfied for any trajectory of θ, if there exists a $\gamma > 0$ and a matrix $P = P^T > 0$ such that for all trajectory of θ in Θ:

$$\begin{bmatrix} A(\theta)^T P + PA(\theta) & PB(\theta) & C(\theta)^T \\ B(\theta)^T P & -\gamma I & D(\theta)^T \\ C(\theta) & D(\theta) & -\gamma I \end{bmatrix} < 0 \qquad (5)$$

Our system is a polytopic LPV, that is to say the varying system is always a barycenter of the linearised systems on the corners of the polytope. Furthermore, if the system is a polytopic LPV system, so does the closed-loop system. As a result:

$A(\theta(t)) = \sum_i \alpha_i(t) A_i$ with $0 \leq \alpha_i(t) \leq 1$ and $\sum \alpha_i(t) = 1$

where A_i are the state matrices of the system on each corner of the polytope. Quadratic stability is satisfied for every trajectory in the polytope if there exists a P positive matrix such that the LMI is satisfied on each corner of the polytope (on linearised systems).

Note that this is only a sufficient condition. This analysis has been performed on the system and it has shown that the system is stable for every arbitrarily variations of ω_{e1} and ω_{e2} in the polytope AB.

5.4 Performance robustness

Stability being checked, it is possible to study performances of our closed-loop system for every variations on the polytope. The system being non-linear, it is useless studying transfer function, so other tools have to be used.

Consider first a LTI system with unit feedback. As already mentioned the sensitivity function $S(j\omega)$ is the transfer between references r and errors ε, and $|S(j\omega_0)|$ (or its maximal singular value for MIMO systems) represents the value of the tracking error when the reference $r(t) = sin(\omega_0 t)$. In a similar way for LPV systems, one would like to compute $S_{LPV}(j\omega_0) = max_{\theta \in \Theta} \|\varepsilon\|_2$ for $r(t) = sin(\omega_0 t)$ which is the maximum energy of the tracking error for all trajectory $\theta(t)$ in the polytope Θ.

It is possible to show that γ obtained resolving 5 is an upper-bound for the H_∞-norm of the system. Let's define the energetic function $V(x) = x^T P x$ and the S-dissipativity function between inputs u and outputs y as:

$$S(u,y) = \begin{pmatrix} y \\ u \end{pmatrix}^T \begin{bmatrix} -I & 0 \\ 0 & \gamma^2 I \end{bmatrix} \begin{pmatrix} y \\ u \end{pmatrix}$$

Then, we have:

$$\frac{d}{dt}V(x) = \begin{pmatrix} x \\ u \end{pmatrix}^T \begin{bmatrix} A(\theta)^T Q + QA(\theta) & QB(\theta) \\ B(\theta)^T Q & 0 \end{bmatrix} \begin{pmatrix} x \\ u \end{pmatrix}$$
$$S(x,y) = \begin{pmatrix} x \\ u \end{pmatrix}^T \begin{bmatrix} -C(\theta)^T C(\theta) & -C(\theta)^T D(\theta) \\ -D(\theta)^T C(\theta) & -D(\theta)^T D(\theta) + \gamma^2 I \end{bmatrix} \begin{pmatrix} x \\ u \end{pmatrix}$$

Substracting each element of the 2 previous equations, and using Schur lemma, it shows that if (5) is satisfied on each corner, then: $\frac{d}{dt}V(x) < S(u,y)$ (see Scherer et al. (2004)). As a result, this S-dissipativity is equivalent to: $\int_0^\infty y^T y < \gamma^2 \int_0^\infty u^T u$, which is the definition of H_∞-norm, valid for a linear as well as a non-linear framework. This tool is very powerful, because it allows getting the H_∞-norm for every variation of θ on the polytope. In this case, γ represent the energetic gain between a random input signal and the corresponding output signal. To get details on performances it is possible to use frequency dependent weights. For example, consider a weight that is null for every frequency except between ω_a and ω_b where its value is 1. The H_∞-norm γ_{ab} of a SISO system with this weight on its input represent the maximum power gain between an input signal whose spectrum is between ω_a and ω_b, and corresponding output. Consider $\omega_a = \omega_b = \omega_0$, then draw $\gamma = f(\omega_0)$. This kind of study can of course be also performed for KS, SG (etc.) functions.

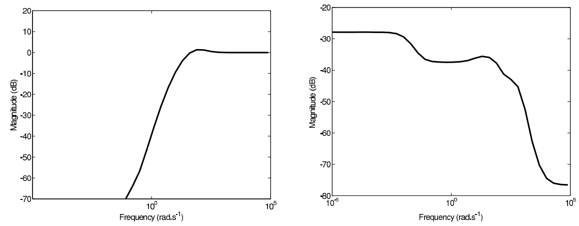

Fig. 7. non-linear S evaluation for Wice (left) and To (right)

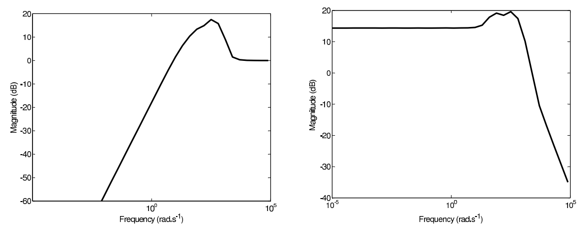

Fig. 8. non-linear S evaluation for Ecapa (left) and non-linear KS evaluation (right)

As an example to understand the use of such a curve, let's consider the closed-loop system with references as inputs and tracking error on ω_{ice} as output. Figure (7 left) is obtained. This curve allows to get the maximum value of the bandwidth for references so that sufficiently small tracking error is obtained. For instance, if the bandwidth is $10 rad.s^{-1}$, the maximum gain between references and error on ω_{ice} is $-10dB$. To study performance on T_o and E_{capa}, figures (7 right) and (8 left) are studied. Figure (8 right) shows the curve obtained considering references as inputs and all control variables as outputs. Because there is no particular link between one reference and one control variable, this curve is global (the system being 3×3, one should consider nine curves to be exhaustive).

Note that it is also possible to use weights on the outputs, but the system being non-linear, the meaning of the curves is not the same. Considering references as inputs and tracking errors as outputs, if a curve has the same shape as (7 left), it shows that for every reference (at any frequency) low error is obtained until a readable frequency. It is also important to note that the transfer function got with the linearised model is smaller than both kinds of curves (with input or output weights).

6. *SIMULATIONS*

The main advantages of this method is the possibility to change specifications very sharply. A controller is designed, whose specifications (based on paragraph 2.1) are:

$\tau_{\omega ice}$	τ_{T_o}	$max(\vert U_{capa}^{ref} - U_{capa}\vert)$
100ms	as small as possible	25V

The aim of this synthesis is to get a controller able to track ω_{ice} during hard simulation events. In order to check the performances of this controller, a complete discrete model of the vehicle is required. Because the system is non-linear, it is not possible to test each scenario and to get exhaustive results. But simulations on the whole polytope give significant results.

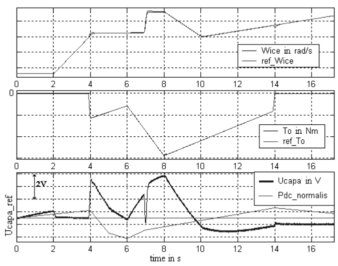

Fig. 9. ω_{ice}, T_o and U_{capa} and references

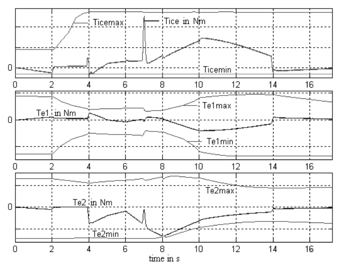

Fig. 10. Actuators torques

Different types of events are simulated. Several values are changed: ω_{ice} and T_o references, $\mathcal{P}_{dcdc}$, and consequently ω_{e1}, ω_{e2} and the vehicle speed. Figure 9 shows ω_{ice}, T_o and U_{capa} and their references. We also draw $\mathcal{P}_{dcnormalis}$, that is equal to $\mathcal{P}_{dcdc}$ divided by its maximum and centered, in order to be easily compared to other variables. Studying T_{e1}, T_{e2} and T_{ice} torques is interesting to check if they remain inside specifications (figure 10). These simulations show that a LTI controller give convenient results.

7. CONCLUSION

The hybrid electric vehicle described in this paper is a potential solution to reduce CO_2 emissions and fuel consumption. This paper aims at describing one way to design controllers satisfying specifications for this powertrain. A two-level control structure has been defined in order to imitate a classic powertrain behavior. Then, a controller has been designed using H_∞ synthesis. To check the robustness of stability and performances, this controller has been analysed with a LPV analysis tool. Since simulation of the closed-loop system gave good results, this control law will be implemented into a prototype. To increase robustness or to adapt such design methods to other systems, it may be useful to design H_∞ LPV-controller.

REFERENCES

A. Villeneuve "Dual mode electric infinitely variable transmission", Aachener kolloquium fahrzeug- und motorentechnik, 2004.

D.J Leith, W.E Leithead "Survey on gain-scheduling analysis and design", Int. journal of control, 2000.

A. Helmersson "Methods for robust gain scheduling", Phd Thesis, Linkping university, 1995.

J.C. Doyle, K. Glover, P.P. Khargonekar, B. Francis "State space solutions for H_2 and H_∞ control problems", IEEE trans. on automatic control, 1989.

P. Gahinet, P. Apkarian, M. Chilali "Affine parameter-dependent Lyapunov functions and real parametric uncertainty", IEEE trans. on automatic control, 1996.

K. Glover, J.C. Doyle "State space formulae for all stabilizing controllers that satisfy an H_∞-norm bound and relations to risk sensitivity", Systems and control letters, 1988.

P. Apkarian, P. Gahinet "A linear matrix inequality approach to H_∞ control", Int. Journal of robust and non linear control, 1994.

K. Zhou, J.C. Doyle, K. Glover *"Robust and optimal control",* Prentice-hall, 1996.

C.W. Scherer, S. Weiland "Course on Linear Matrix Inequalities in Control", http://www.cs.ele.tue.nl/sweiland/lmi.html, 2004.

C.C. Chan, K.T. Chau "Modern Electric and Hybrid Vehicles", Oxford science publications, 2001.

J. Larminie, J. Lowry "Electric Vehicle : Technology Explained", CRC press, 2003.

K.T. Chau, Y.S. Wong "Overview of power management in hybrid electric vehicles", Energy conversion and management 43, 2002.

T. Hofman, R. van Druten "Concept design for hybrid vehicle power systems", American control conference, 2005.

G. Becker, A. Packard "Robust performance of linear parametrically varying systems using parametrically-dependent linear feedback", American control conference, 2005.